

HENRY

Hydraulic Engineering Repository

Ein Service der Bundesanstalt für Wasserbau

Conference Paper, Published Version

Bonelle, S.; Benahmed, N.; Brivois, O. On Modelling of the Hole Erosion Test

Verfügbar unter/Available at: <https://hdl.handle.net/20.500.11970/100003>

Vorgeschlagene Zitierweise/Suggested citation:

Bonelle, S.; Benahmed, N.; Brivois, O. (2006): On Modelling of the Hole Erosion Test. In: Verheij, H.J.; Hoffmans, Gijs J. (Hg.): Proceedings 3rd International Conference on Scour and Erosion (ICSE-3). November 1-3, 2006, Amsterdam, The Netherlands. Gouda (NL): CURNET. S. 107-112.

Standardnutzungsbedingungen/Terms of Use:

Die Dokumente in HENRY stehen unter der Creative Commons Lizenz CC BY 4.0, sofern keine abweichenden Nutzungsbedingungen getroffen wurden. Damit ist sowohl die kommerzielle Nutzung als auch das Teilen, die Weiterbearbeitung und Speicherung erlaubt. Das Verwenden und das Bearbeiten stehen unter der Bedingung der Namensnennung. Im Einzelfall kann eine restriktivere Lizenz gelten; dann gelten abweichend von den obigen Nutzungsbedingungen die in der dort genannten Lizenz gewährten Nutzungsrechte.

Documents in HENRY are made available under the Creative Commons License CC BY 4.0, if no other license is applicable. Under CC BY 4.0 commercial use and sharing, remixing, transforming, and building upon the material of the work is permitted. In some cases a different, more restrictive license may apply; if applicable the terms of the restrictive license will be binding.



On Modelling of the Hole Erosion Test

S.Bonelli*, N. Benahmed* and O. Brivois*,**

* Cemagref/Hydraulics Engineering and Hydrology Research Unit, Aix-en-Provence, France

** CNRS/Mechanics and Acoustics Laboratory, Marseille, France

I. INTRODUCTION

Internal erosion of soil induced by seepage flow is the main cause of major hydraulic works failures (dykes, dams). The issue is defined by the risk of flooding of areas located downstream. When internal erosion is suspected to occur or is already detected in situ, the amount of warning time before failure is difficult to predict. The development of effective emergency action plans which will lead to prevent heavily loss of life and property damage is strongly linked to the knowledge of a characteristic time.

During the last decades, several investigations were carried out to study the internal erosion on the laboratory. Four types of this process were, particularly, identified [4], [5]: 1) evolution of defect (cracks or microfissures) in the soil matrix, 2) regressive erosion, 3) internal suffusion which modifies the soil structure, 4) external suffusion between two soils. This study concerns the first mechanism: the enlargement of a crack which leads to an internal erosion called “piping” in soil mechanics.

Numerous experimental methods have been performed in order to reproduce the internal erosion process in the laboratory and different types of equipment were developed with particular attention focussed on the hole erosion tests [3], [12], [13]. However, few attempts have been made to model these tests. The purpose of this paper is to propose a useful model for the interpretation of the hole erosion test.

On the first part, equations of diphasic flow and equations of jump with erosion are presented. On the second part, a model is developed from spatial integration of a set of simplified equations obtained from asymptotic developments in the case of a circular hole. Some comparison of modelling with experiments are finally shown on the third part.

II. TWO-PHASE FLOW EQUATION WITH INTERFACE EROSION

We study the surface erosion phenomenon of a fluid/soil interface under a flow parallel to the interface. The soil, considered here as saturated, is eroded by the flow which then transports the eroded particles. As far as the particles are smaller enough compared to the characteristic length scale of the flow, this two-phase flow can be considered as a continuum. We note Ω the two-phase mixture volume and Γ the fluid/soil interface. For

simplification, sedimentation and deposition processes are neglected. The mass conservation equations for the water-particles mixture and for the mass of particles as well as the balance equation of momentum of the mixture within Ω can be written as follows in an Eulerian framework [6], [10]:

$$\frac{\partial \rho}{\partial t} + \vec{\nabla} \cdot (\rho \vec{u}) = 0 \quad (1)$$

$$\frac{\partial \rho Y}{\partial t} + \vec{\nabla} \cdot (\rho Y \vec{u}) = -\vec{\nabla} \cdot \vec{J} \quad (2)$$

$$\frac{\partial \rho \vec{u}}{\partial t} + \vec{\nabla} \cdot (\rho \vec{u} \otimes \vec{u}) = \vec{\nabla} \cdot \boldsymbol{\sigma} \quad (3)$$

In these equations, ρ is the density mixture, depending on the particles mass fraction Y ; \vec{u} is the mass-weighted average velocity; \vec{J} is the mass diffusion flux of particles; $\boldsymbol{\sigma}$ is the Cauchy stress tensor in the mixture.

The two media, i.e. the soil and the two-phase fluid, are separated by the interface Γ . The water particles mixture is assumed to flow as a fluid above Γ , while a solid-like behaviour is considered underneath. As erosion occurs, a mass flux crosses this interface and so undergoes a transition from solid-like to fluid-like behaviour. As a consequence, Γ is not a material interface: at different moments, Γ is not defined by the same particles. We assume that Γ is a purely geometric separation and has no thickness. Let us denote by \vec{n} the normal unit vector of Γ oriented outwards the soil, and \vec{v}_Γ the normal velocity of Γ . The jump equations over Γ are [9]:

$$\llbracket \rho(\vec{v}_\Gamma - \vec{u}) \cdot \vec{n} \rrbracket = 0 \quad (4)$$

$$\llbracket \rho Y(\vec{v}_\Gamma - \vec{u}) \cdot \vec{n} \rrbracket = \llbracket \vec{J} \cdot \vec{n} \rrbracket \quad (5)$$

$$\llbracket \rho \vec{u}(\vec{v}_\Gamma - \vec{u}) \cdot \vec{n} \rrbracket = -\llbracket \boldsymbol{\sigma} \cdot \vec{n} \rrbracket \quad (6)$$

This project was sponsored by the Région Provence Alpes Côte d’Azur. This research effort is continuing under the sponsorship of the French National Research Agency under grant 0594C0115 (ERINOH).

where $\llbracket a \rrbracket = a_g - a_b$ is the jump of any physical variable a across the interface, and a_g and a_b stands for the limiting value of a from the solid and fluid sides of the interface, respectively. The soil is supposed homogeneous, rigid and without seepage. The co-ordinate system is linked to the soil. In this case, the total flux of eroded material (both particles and water) crossing the interface is $\dot{m} = -\rho_g \vec{v}_\Gamma \cdot \vec{n}$ where ρ_g is the density of the soil.

Erosion laws, dealing with soil surface erosion by a tangential flow, are often written as threshold laws such as [2]:

$$\dot{m} = k_{er}(|\tau_b| - \tau_c) \text{ if } |\tau_b| > \tau_c, 0 \text{ otherwise} \quad (7)$$

where τ_c is the critical (threshold) shear stress for erosion, k_{er} is the coefficient of soil erosion, and $|\tau_b|$ is the tangential shear stress at the interface defined by

$$|\tau_b| = \sqrt{(\boldsymbol{\sigma} \cdot \vec{n})^2 - (\vec{n} \cdot \boldsymbol{\sigma} \cdot \vec{n})^2} \Big|_b \quad (8)$$

This complete set of equations (1-3) were already used to study different situations of permanent flow (boundary layer and free surface flow) over an erodable ground [1]. Here, these equations can be extended to the study of internal erosion by mean of a spatial integration over Ω .

III. APPLICATION TO PIPING EROSION

We consider a cylinder Ω of length L and radius R (with initial value R_0) (Fig. 1). Reference velocity is $V_{fl} = Q_{fl} / \pi R_0^2$ where Q_{fl} is the initial entrance flow, and flow time is $t_{fl} = R_0 / V_{fl}$. By assuming an axisymmetrical flow, we eliminate one momentum equation. We introduce the small parameter R_e^{-1} to simplify the dimensionless equations in a boundary layer theory spirit [8],[11]. Reynolds number $Re = V_{fl} R_0 / \nu_f$ is assumed to be large, where ν_f is the kinematic viscosity. Navier-Stokes equations are written with the time scaled by t_{fl} , the axial coordinate by $R_0 R_e$, the radial coordinate by R_0 , the axial velocity by V_{fl} , the radial velocity by V_{fl} / R_e , and stresses scaled by $\rho_f V_{fl}^2$. Supposing turbulent stress viscosity and diffusivity, we make regular asymptotic expansion of unknown and we neglect the terms of order $O(R_e^{-1})$ in (1) and (2) (as in [1]). As a result, we have now only one momentum equation, and the pressure is uniform across a section.

Therefore, we integrate the obtained system first on a cross section, and secondly along the axis. We denote the mean value of a in a cross section as $\langle a \rangle_R$, and the mean value in Ω as $\langle a \rangle_\Omega$. The mean longitudinal velocity is $V = \langle u \rangle_R$. The mean density of the fluid is $\bar{\rho} = \langle \rho \rangle_\Omega$. Some assumptions are made: A1) the

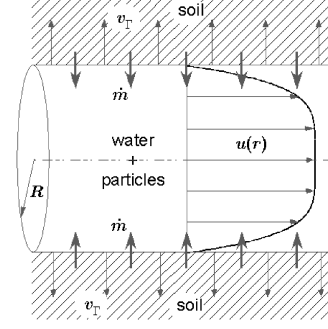


Figure 1. Sketch of the axisymmetrical flow with erosion of the soil and transport of the eroded particles

tangential velocities are supposed continuous across Γ (no-slip condition on the interface), A2) the radial profile of the velocity field is given by the Nikuradze approximation, A3) the concentration is uniform in a section, A4) we introduce a phenomenological friction coefficient f_b by $\tau_b = f_b \bar{\rho} V^2$, A5) the radius R is axially uniform (as a consequence, $V = \langle u \rangle_\Omega$). This leads to an ordinary differential system with unknowns $(R, \bar{\rho}, V)$ which can be solved numerically.

If the erosional time scale is chosen, dimensional analysis reveals that the four basic dimensionless parameters of the system are:

$$\tilde{a}_\phi = \frac{\alpha R_0 \rho_g}{2 f_b L \rho^f}, \tilde{b}_\phi = \left(\frac{\langle u^2 \rangle_\Omega}{\langle u \rangle_\Omega^2} - 1 \right) \left(1 - \frac{\rho^f}{\rho_g} \right) \quad (9)$$

$$\tilde{k}_{ref} = \frac{k_{er} V_{fl}}{1 + k_{er} V_{fl}}, \tilde{\tau}_c = \frac{\tau_c}{P_{fl}} \quad (10)$$

The stress $P_{fl} = R_0(p_{in} - p_{out}) / 2L$ represents the hydraulic gradient and depends on the input and output pressures, respectively p_{in} and p_{out} . The positive dimensionless number $\alpha = (\rho_{out} - \rho_f) / (\bar{\rho} - \rho_f)$ represents the fact that the input fluid is pure water, while the output fluid is a two-phase mixture ($\rho_f < \bar{\rho} < \rho_{out}$).

The erosional velocity appears to be $V_{er} = k_{er} P_{fl} / (1 + k_{er} V_{fl}) \rho_g$. The eroded flow is thus $Q_{er} = 2\pi R_0 L V_{er}$ and the erosional time is $t_{er} = R_0 / V_{er}$. As a consequence, the erosional flow scale ratio is $Q_{er} / Q_{fl} = \alpha \tilde{k}_{ref} \tilde{a}_\phi^{-1}$, the erosional time scale ratio is $t_{fl} / t_{er} = \tilde{k}_{ref} f_b \rho^f / \rho_g$ and the maximum volumic concentration is $c_{ref} = (1 - n) / (1 + \tilde{a}_\phi \tilde{k}_{ref}^{-1})$ where n is the porosity of the soil.

Now we assume that $\tilde{a}_\phi \geq O(1)$ and $\tilde{b}_\phi \approx O(1)$, which is the case in the experiments described below. We call \tilde{k}_{ref} the kinetics of erosion (dimensionless) number. If $\tilde{k}_{ref} \ll 1$ is a small parameter, then asymptotic analysis

leads to important conclusions: 1) the concentration is low and becomes a secondary unknown as it does not influence the density, the inertia, the velocity nor the stress, 2) the flow is quasisteady, 3) the interface velocity is low and does not contribute to inertia. We call this case, which arises when $k_{er} \ll V_{fl}^{-1}$, the situation of low kinetics of erosion.

Starting from initial condition ($R(0) = R_0, V(0) = 0$), and under constant hydraulic gradient $P_{fl} > \tau_c$, the solution of the system can be written as:

$$\frac{R(t)}{R_0} = 1 + \left(1 - \frac{\tau_c}{P_{fl}}\right) \left[\exp\left(\frac{t}{t_{er}}\right) - 1 \right] \quad (10)$$

$$\frac{Q(t)}{Q_{fl}} = \left(\frac{R(t)}{R_0}\right)^{5/2} \quad (11)$$

$$t_{er} = \frac{2L\rho g}{k_{er}(p_{in} - p_{out})} \quad (12)$$

The shear stress at the interface and the velocity are given by

$$\frac{\tau_b(t)}{P_{fl}} = \frac{R(t)}{R_0}, \quad \frac{V(t)}{V_{fl}} = \sqrt{\frac{R(t)}{R_0}} \quad (13)$$

It is important to note that the limiting case $\tilde{k}_{ref} \rightarrow 1$ (corresponding to $k_{er} \rightarrow \infty$) may be of interest. In this case, the concentration can be high, and even more close to the compacity of the soil $c_{ref} = (1 - n) / (1 + \tilde{a}_\phi)$. The erosional law (3) leads to $\tau_b = \tau_c$, but the rheological law depends strongly upon the concentration [7] (assumption A4 has to be modified) so the velocity remains unknown. Moreover, the concentration influences most probably the velocity profile: assumptions A2 and A4 are not relevant anymore. To our knowledge, radial profil of concentration in pipe flow with erosion remains to be

investigated.

IV. COMPARISON WITH EXPERIMENT

According to the logic of the derivation given above, the obtained scaling laws (10) and (11) should hold in all past and future experiments performed in erosional pipe flow with constant pressure drop, in the situation of low kinetics of erosion. The ultimate justification is a comparison with experiment.

The Hole Erosion Test has been designed to reproduce piping flow erosion in a hole [3]. The soil specimen is compacted inside a standard mould used for the Standard Compaction Test. A hole is drilled along the longitudinal axis of the soil sample. An eroding fluid is driven through the soil sample to initiate erosion of the soil along the preformed hole. The test result is described by the flow rate versus time curve under constant pressure drop. For further details on this test, see [3], [12], [13].

The predicted scaling law is now compared to available data produced by [3]. Scaling were performed on 18 tests, concerning 10 different soils (clay, sandy clay, clayey sand or silty sand). Table I contains geological origin, particle size distribution and particle density of soils samples. Table II contains geotechnical properties of soil samples. Table III contains parameters of 18 the hole erosion tests. Table IV contains results of the modelling of these tests with the scaling law (10) and (11). The initial radius and the length of the pipe were $R_0=3$ mm and $L=117$ mm. The range of \tilde{a}_ϕ numbers is 2.37 to 4.82, and the range of \tilde{k}_{er} numbers is $7.54 \cdot 10^{-5}$ to $1.19 \cdot 10^{-2}$, so all cases correspond to the situation of low kinetics of erosion.

Fig. 2 shows the increase of the flow in $Q \propto R^{5/2}$ and shows that the use of t_{er} leads to an efficient dimensionless scaling. In Fig. 3, we plot the experimental data of [3] in the $(R(t)/R_0 - \tau_c/P_{fl}, t/t_{er} + \ln(1 - \tau_c/P_{fl}))$ plane. We observe that all the data except for few fall on a single curve. Taking into account the many simplifying assumptions, the agreement with the scaling law (4) speaks for itself: in spite of the large range of k_{er} (three orders of magnitude), no further manipulation is needed to bring its consequences into line with the experimental data.

TABLE I.
GEOLOGICAL ORIGIN, PARTICLE SIZE DISTRIBUTION AND PARTICLE DENSITY OF SOIL SAMPLES

Soil	Geological Origin	%Gravel	%Sand	%Fines	%Finer than 0.002mm	Soil Particle Density
Bradys	Residual	1	24	75	48	2.74
Fattorini	Colluvial	3	22	75	14	2.68
Hume	Alluvial	0	19	81	51	2.71
Jindabyne	Residual	0	66	34	15	2.68
Lyell	Residual	1	70	29	13	2.61
Matahina	Residual	7	43	50	25	2.67
Pukaki	Glacial	10	48	42	13	2.70
Shellharbour	Residual	1	11	88	77	2.75
Waranga	Alluvial	0	21	79	54	2.69

TABLE II.
GEOTECHNICAL PROPERTIES OF SOIL SAMPLES

Soil		Test Name	Optimum Water Content (%)	Test Water Content (%)	Optimum Porosity	Test Porosity
Bradys	high plasticity sandy clay	BDHET001	35.0	35.8	0.52	0.52
		BDHET002	35.0	35.9	0.52	0.52
Fattorini	medium plasticity sandy clay	FTHET010	18.5	15.6	0.37	0.37
Hume	low plasticity sandy clay	HDHET001	21.0	21.4	0.39	0.40
		HDHET005	21.0	17.9	0.39	0.40
		HDHET006	21.0	22.6	0.39	0.40
		HDHET007	21.0	22.4	0.39	0.40
		HDHET009	21.0	22.7	0.39	0.40
Jindabyne	clayey sand	JDHET001	16.0	15.7	0.35	0.35
		JDHET005	16.0	13.8	0.35	0.35
		JDHET013	16.0	16.2	0.35	0.35
		JDHET016	16.0	18.3	0.35	0.35
Lyell	silty sand	LDHET014	10.0	8	0.25	0.25
Matahina	low plasticity clay	MDHET006	16.5	14.3	0.32	0.32
Pukaki	silty sand	PDHET003	8.5	8.6	0.20	0.20
Shellharbour	high plasticity clay	SHHET005	41.0	38.7	0.55	0.55
		SHHET009	41.0	37.9	0.55	0.55

V. CONCLUSION

Many laboratory tests are commonly used to study internal erosion in a soil. One of them, the hole erosion test appears to be efficient and simple to quantify the rate of piping erosion, but few attempts have been made to model this test. We started from the field equations of diphasic flow with diffusion, and the equations of jump with erosion. After many simplifying assumptions, from asymptotic developments and dimensionnal analysis, we proposed some characteristic numbers, among which the two most significant are the kinetics of erosion dimensionless number and the erosional time.

We defined a particular case: the situation of low kinetics of erosion. This situation arises when kinetics of erosion is much small than one. In this case, the influence of both concentration and inertial effects can be neglected. We obtained an analytical scaling law for the interpretation of the hole erosion test with constant pressure drop. We made comparison with available experimental data on seventeen tests concerning nine different soils. This comparison has confirmed the validity of our scaling law, which can be used for the interpretation of the hole erosion test.

More research works are needed to investigate if this characteristic time could be used in practical situations to predict the developpement of internal erosion on hydraulic works.

ACKNOWLEDGMENT

The authors wish to thanks Pr. Robin Fell and Dr. Chi Fai Wan for their valuable experimental data.

REFERENCES

- [1] O. Brivois, *Contribution to strong slope erosion by a two-phase turbulent flow*, PhD, University of Aix-Marseille II, 2005.
- [2] H. Chanson, *The Hydraulics of Open Channel Flows: An Introduction*, Butterworth-Heinemann, Oxford, UK, 1999.
- [3] R. Fell and C.F. Wan, *Investigation of internal erosion and piping of soils in embankment dams by the slot erosion test and the hole erosion test* UNICIV Report No R-412, The University of New South Wales Sydney ISSN 0077 880X, 2002.
- [4] M. A. Foster and R. Fell, Assessing embankment dam filters that do not satisfy design criteria. *Journal of Geotechnical and Geoenvironmental Engineering*, 127(5), 398–407, 2001.
- [5] J.-J. Fry, *Internal Erosion: Typology, Detection, Repair, Barrages and Reservoirs* No. 6. French Comitee of Large Dams, Le Bourget-du-lac Cedex, 1997.
- [6] P. Germain, Q.S. Nguyen and P. Suquet, Continuum Thermodynamics, *Journal of Applied Mechanics*, 50, 1010-1020, 1983.
- [7] P.-Y. Julien, *Erosion and Sedimentation*, Cambridge University Press, 1995.
- [8] P.-Y. Lagrée and S. Lorthois, The RNS/Prandtl equations and their link with other asymptotic descriptions. Application to the computation of the maximum value of the Wall Shear Stress in a pipe, *International Journal of Engineering Science*, 43(3), 352-378, 2005.
- [9] L. W. Morland and S. Sellers, Multiphase mixtures and singular surfaces, *International Journal of Non-Linear Mechanics*, 36, 131-146, 2001.
- [10] R.I. Nigmatulin, *Dynamics of multiphase media*, Book News, Inc. Portland, 1990.
- [11] H. Schlichting, *Boundary layer theory*, 7th ed Mc Graw Hill, New York, 1987.
- [12] C.F. Wan and R. Fell, Investigation of rate of erosion of soils in embankment dams, *Journal of Geotechnical and Geoenvironmental Engineering*, 30(4), 373-380, 2004.
- [13] C.F. Wan and R. Fell, Laboratory Tests on the Rate of Piping Erosion of Soils in Embankment Dams, *Journal of Geotechnical Testing Journal*, 27(3), 2004.

TABLE III.
PARAMETERS OF THE HOLE EROSION TEST

Test	P_{jt} (Pa)	V_{jt} (m/s)	t_{jt} (10^{-3} s)	f_b (10^{-2})	R_e	\tilde{a}_ϕ
BDHET001	79.96	2.20	1.36	1.65	6610	2.84
BDHET002	53.22	1.87	1.61	1.52	5606	3.07
FTHET010	93.78	2.57	1.17	1.42	7721	3.61
HDHET001	92.87	2.43	1.23	1.57	7298	3.30
HDHET005	66.13	2.22	1.35	1.34	6663	3.75
HDHET006	79.30	2.29	1.31	1.51	6875	3.46
HDHET007	79.43	2.33	1.29	1.47	6981	3.56
HDHET009	79.57	2.15	1.39	1.72	6452	3.04
JDHET001	77.74	2.26	1.33	1.53	6769	3.47
JDHET005	9.65	0.71	4.25	1.94	2115	2.68
JDHET013	53.22	1.52	1.98	2.32	4548	2.29
JDHET016	6.91	0.63	4.73	1.72	1904	3.15
LDHET014	7.96	0.81	3.70	1.21	2433	4.57
MDHET006	129.00	2.93	1.03	1.51	8779	3.57
PDHET003	16.43	1.02	2.93	1.57	3067	3.87
SHHET005	106.30	2.68	1.12	1.48	8038	3.05
SHHET009	102.39	2.71	1.11	1.39	8144	3.23
WBHET001	105.91	2.71	1.11	1.44	8144	3.58

TABLE IV.
RESULTS OBTAINED WITH THE SCALING LAW

Test	τ_c (Pa)	V_{er} (10^{-5} m/s)	t_{er} (s)	c_{ref} (10^{-5})	k_{er} (10^{-4} s/m)	$k_{er} V_{jt}$ (10^{-4})
BDHET001	76.07	1.35	223	11	3.02	6.65
BDHET002	50.93	1.43	210	14	4.80	8.97
FTHET010	6.63	4.10	73	39	8.57	22.05
HDHET001	92.87	0.94	319	9	2.01	4.88
HDHET005	66.13	1.00	299	10	2.93	6.50
HDHET006	76.00	0.18	1712	2	0.44	1.01
HDHET007	79.41	0.50	600	5	1.26	2.93
HDHET009	74.42	0.14	2183	1	0.35	0.75
JDHET001	72.32	2.26	133	25	5.89	13.30
JDHET005	6.92	0.46	647	16	9.59	6.76
JDHET013	49.66	0.79	380	13	3.03	4.59
JDHET016	6.42	0.26	1165	10	7.73	4.90
LDHET014	7.95	5.22	57	185	139.19	112.86
MDHET006	128.22	0.71	424	6	1.13	3.31
PDHET003	13.85	0.71	424	21	10.05	10.28
SHHET005	106.20	1.98	152	13	3.22	8.63
SHHET009	99.77	0.31	975	2	0.52	1.40
WBHET001	105.81	1.41	213	12	2.62	7.12

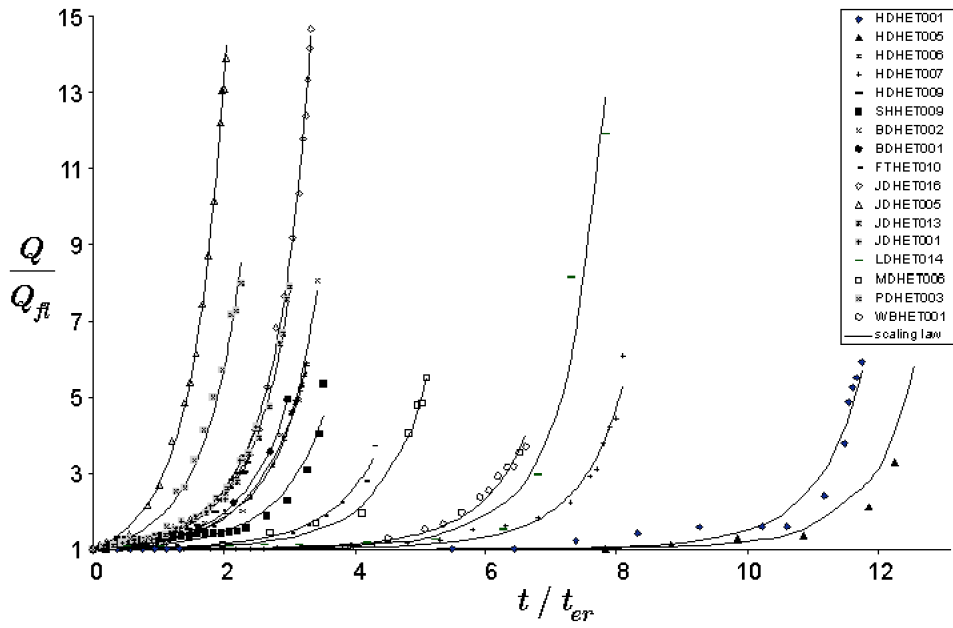


Figure 2. Hole Erosion Test, data(symbols)/ scaling law (continuous lines) comparison, dimensionless flow as a function of dimensionless time. The experimental data are taken from [2].

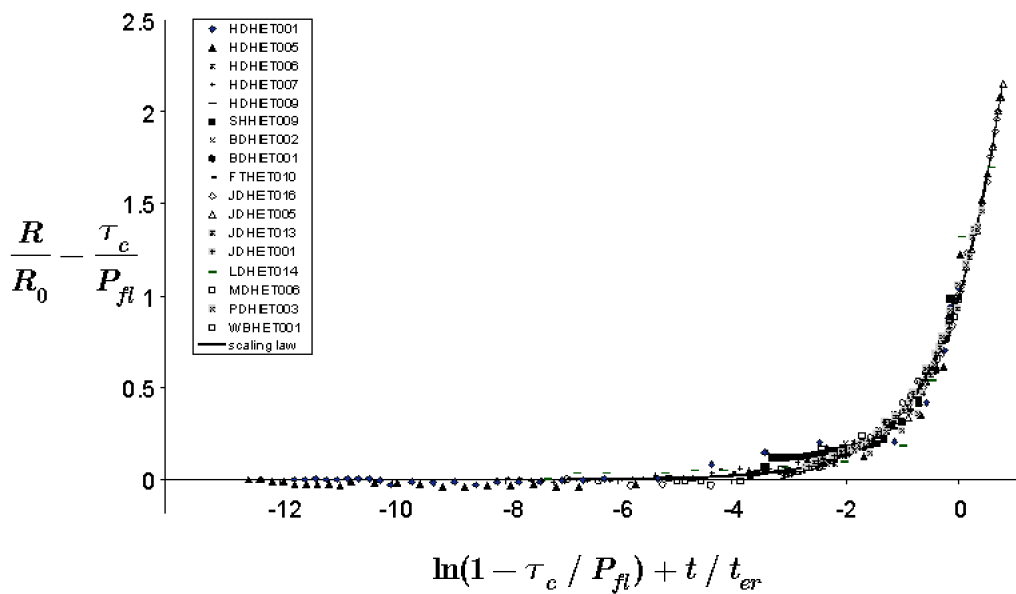


Figure 3. Hole Erosion Test, data(symbols)/scaling law(continuous lines) comparison, dimensionless radius as a function of dimensionless time. The experimental data are taken from [2].